FEBS Letters 588 (2014) 2881–2889

journal homepage: www.FEBSLetters.org

Gatekeeper tyrosine phosphorylation is autoinhibitory for Symbiosis Receptor Kinase

Anindita Paul [a,1], Sandip Samaddar [a,1], Avisek Bhattacharya [a], Anindyajit Banerjee [b], Abhishek Das [b], Saikat Chakrabarti [b], Maitrayee DasGupta [a,*]

[a] Department of Biochemistry, University of Calcutta, Kolkata, India
[b] Indian Institute of Chemical Biology, 4, Raja S.C. Mullick Road, Kolkata 700 032, India

ARTICLE INFO

Article history:
Received 24 April 2014
Revised 19 June 2014
Accepted 23 June 2014
Available online 1 July 2014

Edited by Julian Schroeder

Keywords:
Gatekeeper tyrosine
Autophosphorylation
Autoinhibition
Symbiosis Receptor Kinase

ABSTRACT

Plant receptor-like kinases (RLKs) are distinguished by having a tyrosine in the 'gatekeeper' position. Previously we reported Symbiosis Receptor Kinase from *Arachis hypogaea* (*Ah*SYMRK) to autophosphorylate on the gatekeeper tyrosine (Y670), though this phosphorylation was not necessary for the kinase activity. Here we report that recombinant catalytic domain of *Ah*SYMRK with a phosphomimic substitution in the gatekeeper position (Y670E) is catalytically almost inactive and is conformationally quite distinct from the corresponding native enzyme. Additionally, we show that gatekeeper-phosphorylated *Ah*SYMRK polypeptides are inactive and depletion of this inactive form leads to activation of intramolecular autophosphorylation of *Ah*SYMRK. Together, our results suggest gatekeeper tyrosine autophosphorylation to be autoinhibitory for *Ah*SYMRK.

Structured summary of protein interactions:
AhSYMRK and **AhSYMRK** bind by molecular sieving (1, 2)
AhSYMRK and **AhSYMRK** phosphorylate by protein kinase assay (View interaction)

1. Introduction

Gatekeeper position in protein kinases is located on a conserved β5 strand, distal to the active site and is adjacent to an intrinsically flexible hinge region that connects the N- and C-terminal lobes of the enzyme [1–3]. The position is referred to as a gatekeeper because it flanks a hydrophobic pocket at the rear of the catalytic cleft and confers selectivity for binding nucleotides and small-molecule inhibitors in the pocket [4,5]. Apart from being the architect of this deep cleft, gatekeeper position has gained more importance because several evidences indicate that protein kinases have adopted different mechanisms of regulation mediated by their respective gatekeeper residue and/or the hinge region [4,6]. Bulkier hydrophobic residue at gatekeeper position has been shown to activate tyrosine kinases whereas smaller residue, like glycine, causes inactivation [6]. Structural analysis suggested that the bulkier residue stabilises the active conformation by strengthening a 'hydrophobic spine', whereas the smaller residue inactivates the kinase by disruption of the same hydrophobic connectivity [4]. Emrick et al. had demonstrated the role of the gatekeeper residue in restraining auto-activation of ERK2 in the absence of upstream signalling [7]. Recent evidences have directly demonstrated that backbone flexibility within the hinge region adjacent to gatekeeper residue is an important determinant of ERK2 activation [8].

Plant receptor-like kinases (RLKs) and receptor-like cytoplasmic kinases (RLCKs) share a common feature with the animal interleukin-1 receptor-associated kinase (IRAK)/Pelle family of soluble kinases that distinguishes them from all other kinases: the presence of a Tyr residue in their gatekeeper position [9]. Several evidences have indicated the importance of gatekeeper tyrosine in determining the active conformation of these receptor or non-receptor kinases. In IRAK4, the invariant glutamate from α-helix C forms hydrogen bonds with gatekeeper Tyr as well as the Phe residue in the DFG motif, suggesting the importance of gatekeeper Tyr in regulation of this kinase [10,11]. Structural analysis of gatekeeper residue arrangement in BRASSINOSTEROID-INSENSITIVE 1 (BRI1) and BRI1-associated kinase 1 (BAK1) of *Arabidopsis thaliana*

Abbreviations: RLK, receptor-like kinase; RTK, receptor tyrosine kinase; IRAK, interleukin-1 receptor-associated kinase; SYMRK, Symbiosis Receptor Kinase; WT, wild-type; Trx, thioredoxin; CD, circular dichroism

* Corresponding author.
E-mail address: maitrayee_d@hotmail.com (M. DasGupta).

[1] These authors contributed equally.

http://dx.doi.org/10.1016/j.febslet.2014.06.056
0014-5793/

suggests that hydrogen-bond interactions of the hydroxyl group of the invariant gatekeeper tyrosine with the conserved Lys/Glu salt-bridge (residue 911/927 and 317/334 in BRI1 and BAK1, respectively) are hall-marks of activated plant receptor-like kinases [12,13]. The importance of gatekeeper tyrosine in the functional outputs of RLKs/RLCKs is also evidenced. For example, structure–mimic substitutions of gatekeeper Tyr–Phe in BRI1 (Y956F) [14], or in an RLCK like Botrytis-induced kinase 1 (BIK1, Y150F) [15], blocks their *in vitro* kinase activity as well as biological function. In lysin motif domain-containing receptor like kinase-3 (LYK3), a gatekeeper mutant (Y390F) retained partial kinase activity, but mutant LYK3 was biologically active [9]. In contrast, in gatekeeper mutants Y363F of BAK1 [16] or Y670F of Symbiosis Receptor Kinase of *Arachis hypogaea* [17], the catalytic potential of the RLKs remain unaffected. This indicates that unlike BRI1 or BIK1, for RLKs like SYMRK or BAK1, the H-bonding network involving the free hydroxyl group of gatekeeper tyrosine was not essential for their *in vitro* catalytic activity. Considering the contrasting effects of gatekeeper substitution in RLKs, the involvement of free hydroxyl group of gatekeeper tyrosine in an H-bonding network cannot be considered as a quintessential signature of the activated state for all RLKs.

Symbiosis Receptor Kinase (SYMRK) is an orphan RLK involved in root nodule symbiosis [18,19]. Earlier, we have demonstrated that gatekeeper Tyr (Y670) is the predominant site of tyrosine autophosphorylation in *A. hypogaea* SYMRK (*Ah*SYMRK) both *in vitro* and *in planta* [17]. Catalytic activity of Y670F mutant of *Ah*SYMRK, indicated that autophosphorylation on gatekeeper Tyr was not a prerequisite for *Ah*SYMRK to be an active kinase [17]. Here we report that recombinant catalytic domain of *Ah*SYMRK with a phosphomimic substitution in the gatekeeper position (Y670E) is conformationally distinct with an almost loss of catalytic activity. We also show that the gatekeeper-phosphorylated *Ah*SYMRK polypeptides were almost inactive indicating that the negative charge of the phosphate group negatively affects the catalytic activity of *Ah*SYMRK. Depletion of this inactive form activated intramolecular autophosphorylation of *Ah*SYMRK, suggesting gatekeeper tyrosine autophosphorylation to be autoinhibitory for this RLK.

2. Experimental procedures

2.1. Cloning, mutagenesis, expression and purification of recombinant AhSYMRK

Amplification, sub-cloning, mutagenesis, expression and purification of recombinant *Ah*SYMRK kinase domain polypeptides were performed as described previously [17]. The primers used for developing Y670E mutant were F-5′GATTCTCGTGGAGCCTTTTAT GTC3′ and B-5′GACATAAAAGGCTCCACGAGAATC3′. Purification of *Ah*SYMRK and its mutant polypeptides through FPLC was performed on Superose 6 10/300 GL column (GE Healthcare) at a flow rate of 0.5 ml/min using a buffer containing 25 mM Tris–HCl at pH 8.0, 150 mM NaCl and 2.5 mM EDTA and 250 μl fractions were collected. Standards for the gel-filtration column (Gel Filtration Calibration Kit, GE Healthcare) were Ferritin (440 kDa), Aldolase (158 kDa), Ovalbumin (44 kDa), and Carbonic Anhydrase (29 kDa). Eluted fractions corresponding to each peak were collected and distributed into 25 μl aliquots, quickly frozen in dry ice and stored at −80 °C for further analysis.

2.2. Kinase assay and phosphoamino acid analysis

Kinase autophosphorylation assays were carried out as described earlier [17,20,21]. Immunoblotting was conducted as per manufacturer's instructions with monoclonal α-pY (1:3000) and polyclonal α-pT (1:3000) from Cell Signaling Technology, polyclonal α-His_6 (1:2000) and monoclonal α-pS Q5 (1:100) from Qiagen, polyclonal α-SYMRK (raised in rabbit against the cytosolic domain of *Ah*SYMRK as described earlier [22]) and custom-made antibody against the synthetic peptide (665-QQILVpYPFMS-674) (Imgenex India) [17]. To monitor the phosphorylation status, Pro-Q Diamond Phosphoprotein Stain (Invitrogen) was used according to manufacturer's protocol and data were obtained using Typhoon Trio+ Scanner (GE Heathcare).

2.3. Circular dichroism (CD)

His_6-*Ah*SYMRK (wild-type (WT)) and its mutants (Y670F, Y670E and K625E) were dialyzed overnight against 5 mM Tris–HCl (pH 8.0) and 25 mM NaCl at 4 °C. Far-UV spectra with excitation wavelengths ranging from 200 to 260 nm were recorded for each protein (final concentration 0.1 mg/ml) in Jasco J-815 CD Spectrometer, in a 0.1 cm path length cuvette. The results were expressed in Molar Ellipticity [23].

2.4. Fluorescence measurements

*Ah*SYMRK and its mutants were dialyzed overnight against 5 mM Tris–HCl (pH 8.0) and 25 mM NaCl and were brought to A_{280} of 0.1 O.D. Measurements were conducted in a 1 cm cuvette at room temperature in a Cary Eclipse Fluorescence Spectrophotometer (Varian). Scans were performed at an excitation wavelength of 280 nm, a bandwidth of 5 nm with a scan speed of 240 nm/min [24].

2.5. Limited proteolysis

For limited proteolysis with trypsin, 40 μg of purified protein was diluted to 250 μl reaction volume containing 50 mM NH_4HCO_3, pH 7.8 and incubated at 37 °C with Trypsin (Promega) at a 1:1000 (w/w) enzyme: substrate ratio [24]. 25 μl aliquots were removed at fixed time points, and the reaction was stopped by the addition of 2X Laemmli buffer and boiling for 5 min. Digested protein samples (~4 μg/lane) were separated in a 7.5% SDS–PAGE and gels were stained with Commassie Brilliant blue R250.

2.6. Immunoprecipitation

*Ah*SYMRK expressed in *Escherichia coli* was immunoprecipitated with monoclonal α-pY antibody (Cell Signaling Technology) under binding conditions described previously with modifications [21]. In brief, 400 μg of protein was incubated in a total reaction volume of 300 μl in the presence of 20 mM HEPES pH 7.4, 150 mM NaCl and 1 μg of the corresponding antibody. Incubation was performed for 4 h at 4 °C. Protein A Sepharose Fast Flow beads (GE Healthcare) were added, gently mixed for 1 h and washed five times with 20 mM HEPES pH 7.4 and 150 mM NaCl. The bound *Ah*SYMRK from the immunoprecipitate was eluted with 2 M NaCl and immediately desalted. 0.2–0.5 μg of the bound and unbound fractions were used for immunoblotting and kinase activity assay.

2.7. Homology modeling analysis

*Ah*SYMRK kinase domain sequence (Uniprot ID: E6YC17) was subjected to HHPRED [25] server for the prediction of secondary and tertiary structure. Fold prediction results suggest strong structural similarity between *Ah*SYMRK kinase domain and human IRAK4 kinase domain complexed with AMPPNP (PDB ID: 2OID; chain B) [11]. Three-dimensional (3D) coordinates of *Ah*SYMRK was generated by MODELLER 9.8 [26] package using chain B of

2OID as ligand bound ('active') reference structure. 3D models were filtered based on the best energy parameters (MOLPDF and DOPE scores) and were further validated using PROCHECK [27] and Verify 3D [28] structure validation tools. Phospho-transfer was performed using the CHIMERA software [29].

3. Results and discussion

3.1. Phosphomimic substitution in gatekeeper position (Y670E) strongly reduces AhSYMRK activity

To clarify the consequence of gatekeeper Tyr phosphorylation on *Ah*SYMRK activity we initiated our investigation by making a phosphomimic substitution of gatekeeper Tyr with Glu (Y670E) in the His_6-tagged core kinase domain (573–883 [17]) of *Ah*SYMRK. The idea was to check the effect of having negative charges in the gatekeeper position buried in the hydrophobic pocket of the catalytic cleft. The mutant polypeptide was expressed and subjected to kinase reaction *in vitro* in presence of [γ-^{32}P]-ATP. The gatekeeper substituted Y670F mutant was used as a control as there is no loss of activity in Y670F *Ah*SYMRK [17]. As indicated in Fig. 1A, the wild-type *Ah*SYMRK and the Y670F mutant actively autophosphorylated but the activity of Y670E kinase was severely affected. Thus a phosphomimic (Y670E) but not a structure-mimic (Y670F) substitution in the gatekeeper position has adverse effect on the catalytic activity of *Ah*SYMRK. In our previous report, we have shown that *Ah*SYMRK autophosphorylated in *E. coli* before extraction [17] and to check the same in Y670E *Ah*SYMRK, we harvested *E. coli* cells overexpressing the polypeptide under denaturing conditions in presence of 8 M urea before purification. As indicated in Fig. 1B, pTyr was undetectable in both the gatekeeper mutants Y670E and Y670F indicating that these mutants were unable to autophosphorylate on tyrosine residues. This observation is also in consistence with gatekeeper Y670 being the primary site of tyrosine phosphorylation in *Ah*SYMRK [17]. pThr and pSer was detectable in both the gatekeeper mutants though the level of autophosphorylation was much lower in Y670E mutant kinase. This indicates that Y670E can autophosphorylate on Ser/Thr but its ability to phosphorylate on tyrosine residues is abolished.

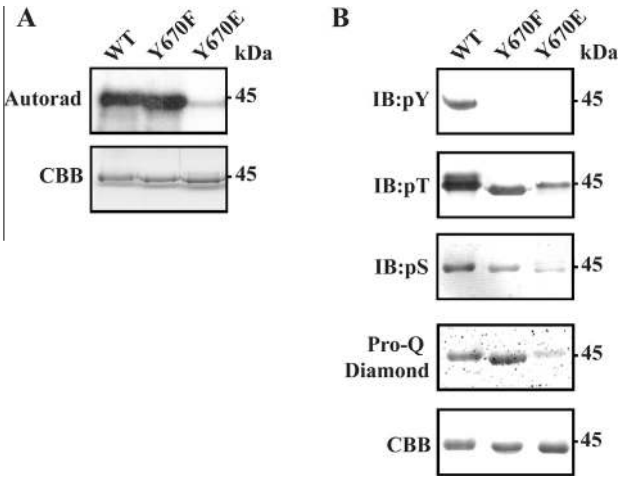

Fig. 1. Phosphomimic substitution in gatekeeper position (Y670E) substantially reduces *Ah*SYMRK activity. (A) Post purification catalytic activity of recombinant *Ah*SYMRK and its gatekeeper mutants Y670F and Y670E: autoradiographs for autophoshorylation. (B) Pre purification phosphorylation status of *Ah*SYMRK and its gatekeeper mutants in *E. coli*: immunoblot analysis using α-pY, α-pT and α-pS antibodies and staining using Pro-Q diamond phosphoprotein stain. (Autorad, autoradiograph; CBB, coomassie brilliant blue; α-pS, anti-phosphoserine; α-pT, anti-phosphothreonine; α-pY, anti-phosphotyrosine.)

Finally, in accordance with Y670E having reduced catalytic activity, phosphoprotein stain indicated the phosphorylation level in Y670E to be very low as compared to WT SYMRK as well as the Y670F mutant. These data indicated that negative charge in the gatekeeper position adjacent to the hinge region of *Ah*SYMRK adversely affects its catalytic activity. This could either be because the negative charge has a destabilizing effect on the ATP-binding cleft of the catalytic groove or the charged residue in the gatekeeper position could also interfere with the hinge-bending motions of the two lobes that are needed for adopting the catalytically competent conformation of protein kinases [30]. Whatever be the case, the gatekeeper residue does not appear to be directly involved in the catalytic phosphotransfer by *Ah*SYMRK since catalytic activity in Y670E was not abolished like the K625E mutant, where the ATP-binding invariant lysine was substituted with Glu [17]. Also, the activity of Y670F mutant clearly showed that neither autophosphorylation on gatekeeper tyrosine (Y670) nor availability of free hydroxyl group of Y670 was necessary for *Ah*SYMRK activity.

3.2. AhSYMRK (Y670E) is conformationally distinct

The native as well as the Y670E kinase domains were analysed using spectroscopy and limited proteolysis to test the effect of phosphomimic substitution at gatekeeper position on the conformation of *Ah*SYMRK. The far-UV circular dichroism spectra of WT *Ah*SYMRK and the gatekeeper mutants, Y670F and Y670E, had negative bands at 208 and 222 nm (Fig. 2A) which is similar to the spectra reported for other receptor tyrosine kinases and supports the ordered helical structure present in the core kinase domain of *Ah*SYMRK [24,31,32]. The spectral overlap between the active kinases (WT and Y670F) and the gatekeeper mutant with strongly reduced activity (Y670E) indicated that there was no significant variation in the secondary structure of the kinase associated with its level of activation. The catalytically dead K625E mutant of *Ah*SYMRK also showed an overlapping spectrum with very small and subtle changes implying that activation of *Ah*SYMRK polypeptide is not associated with any significant change of its secondary structure. As opposed to this, variation in intrinsic tryptophan fluorescence emission (Fig. 2B) was indicative of the conformational variations of active and inactive *Ah*SYMRK polypeptides. The fluorescence was enhanced and red shifted in Y670E (λ_{max} = 347 nm), Y670F (λ_{max} = 348 nm), and WT (λ_{max} = 347 nm) in comparison to the catalytically dead unphosphorylated K625E (λ_{max} = 344 nm). As phosphorylation status is indicative of kinase activity, the relatively less fluorescence emission of Y670E as compared to WT or Y670F is in consistence with its strongly reduced (but not abolished) catalytic activity. The conformations of *Ah*SYMRK polypeptides were further studied using limited proteolysis to probe into the accessibility in protein structure [33]. As shown in Fig. 2C, the trypsin digestion patterns of WT *Ah*SYMRK revealed that the 45 kDa band remained almost undigested after 15 min. In contrast, in the catalytically dead kinase (K625E) the 45 kDa band completely disappeared within 15 min with the concomitant appearance of two visible bands at 42 kDa and 38 kDa indicating this polypeptide to be completely digested under identical conditions. These observations suggest that the native *Ah*SYMRK with a phosphorylated backbone has a rigid structure that is inaccessible to proteases but the catalytically dead unphosphorylated *Ah*SYMRK (K625E) has enhanced backbone flexibility that increased its susceptibility to proteases. In contrast to these extremes, in both the gatekeeper mutants (Y670F and Y670E) the 45 kDa was partially digested after 15 min giving rise to the 42 kDa and 38 kDa bands indicating that these mutants have restricted accessibility to trypsin. Thus both the gatekeeper mutants have more backbone flexibility than the WT *Ah*SYMRK

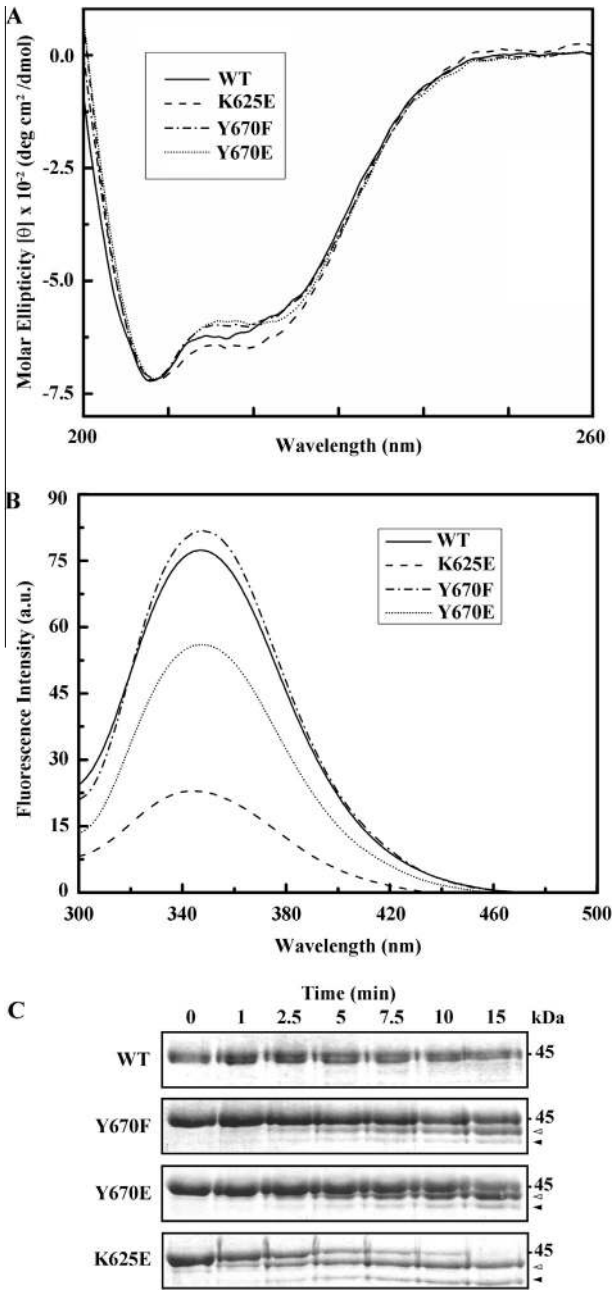

Fig. 2. Conformational analysis of *Ah*SYMRK and its mutant polypeptides. (A) An overlay of the far-UV CD spectra of *Ah*SYMRK and its mutants (WT—, K625E– – –, Y670F–·–·–, Y670E·····). (B) The intrinsic fluorescence spectra of WT—, K625E– – –, Y670F–·–·– and Y670E····· polypeptides were recorded from 300 to 500 nm with an excitation wavelength at 280 nm. (C) Tryptic fingerprinting (at 1:1000 (w/w) enzyme to substrate ratio) of WT, Y670F, Y670E and K625E were done for indicated time points, followed by analysis in a 7.5% SDS–PAGE. Appearance of 42 kDa and 38 kDa bands are indicated with white and black arrowheads, respectively.

but more rigidity as compared to the catalytically dead K625E polypeptide. It is of note that the gatekeeper mutants Y670F and Y670E have similar backbone flexibility in spite of having contrasting catalytic potential.

In summary, in consistence with reduced catalytic potential of Y670E mutant of *Ah*SYMRK, both intrinsic fluorescence emission properties and protease accessibility indicated this polypeptide to be conformationally distinct from both the active WT *Ah*SYMRK as well as its catalytically dead (K625E) counterpart.

3.3. The propensity to oligomerise/dimerise in native AhSYMRK is severely affected in Y670E mutant

Earlier reports indicated that intracellular domains of RLKs possess an intrinsic propensity to form dimers and higher-order oligomers [12,24]. We intended to check whether the native *Ah*SYMRK kinase domain shared this property of dimerisation and/or oligomerisation and if yes, whether Y670E with a distinct conformation differed with respect to the propensity of oligomerisation. The Ni–NTA enriched *Ah*SYMRK polypeptide was clarified through size exclusion chromatography in a Superose 6 column (GE Healthcare). WT *Ah*SYMRK eluted predominantly at around 76 kDa (peak at 16.5 ml) where the catalytically inactive K625E *Ah*SYMRK eluted at around 40 kDa (peak at 17.28 ml) (Fig. 3A and Supplemental Fig. S1), suggesting the active WT polypeptide to be stable in a dimeric form. The monomeric form of K625E polypeptide ruled out the possibility of any influence of the His_6-tag on the dimerisation of *Ah*SYMRK kinase domain (Fig. 3A). We noticed that with increasing concentrations around 75 μM, the WT polypeptide showed an increased tendency to oligomerise and form aggregates that eluted within void volume. This indicated that the WT *Ah*SYMRK had a propensity to oligomerise and this propensity was concentration-dependent. Western blot analysis by α-His_6 as well as α-SYMRK confirmed that the void volume fraction as well as other fractions eluting at higher molecular weight, consisted of aggregates of the WT *Ah*SYMRK polypeptide (Fig. 3B). The void fractions were pooled as Peak1 (P1) and the dimeric fractions as Peak2 (P2) and both were subjected to *in vitro* autophosphorylation assay. As indicated in Fig. 3C, no autophosphorylation was detected in the void fraction (P1) of *Ah*SYMRK. We also tested the fractions eluting in between P1 and P2 containing higher order oligomeric fractions (data not shown), but autophosphorylation was only detectable in the dimeric fraction of *Ah*SYMRK. Immunoblot analysis of P1 and P2 using α-pY670 (665–674) and α-pY indicated that both the oligomeric and dimeric fractions of WT *Ah*SYMRK were autophosphorylated on gatekeeper tyrosine. This indicated that *Ah*SYMRK could actively autophosphorylate on gatekeeper tyrosine before oligomerising into inactive higher order structures. Immunoblot analysis also indicated that all higher order oligomeric structures of *Ah*SYMRK eluting in between P1 and P2 were phosphorylated on gatekeeper tyrosine (data not shown). In summary, our experiments suggested that the catalytic domain of native *Ah*SYMRK existed as a dimer and possessed an intrinsic propensity to form higher-order oligomers. Since we only used the kinase domain for our experiments the observed formation of the dimer or the higher order structures were not contributed by the juxtamembrane region (JM) or the C-terminal (CT) region. This ligand independent formation of dimers by intracellular domains of receptor kinases have been noted earlier; for example, receptor tyrosine kinases (RTKs) such as NGFR, EGFR, and EpoR can exist as preformed dimers even in the absence of ligand [34–38]. Among RLKs, BRI1 [39–41] and the S-locus receptor kinase [42] have been shown to exist as ligand-independent dimers, but the precise mechanism of dimer/oligomer formation in plant RLKs and their *in vivo* relevance remains to be understood.

Our next objective was to check the propensity of oligomerisation in the gatekeeper-substituted Y670E and Y670F mutants (Fig. 3A). For this, the Ni–NTA enriched mutant polypeptides at 75 μM concentration were clarified through size exclusion chromatography in a Superose 6 column under identical conditions. As opposed to the native enzyme that eluted in dimeric form, both the gatekeeper mutants appeared to elute as monomers (Fig. 3A). The Y670E mutant eluted at 17.23 ml along with the catalytically inactive K625E polypeptide at around ~40 kDa (Supplemental

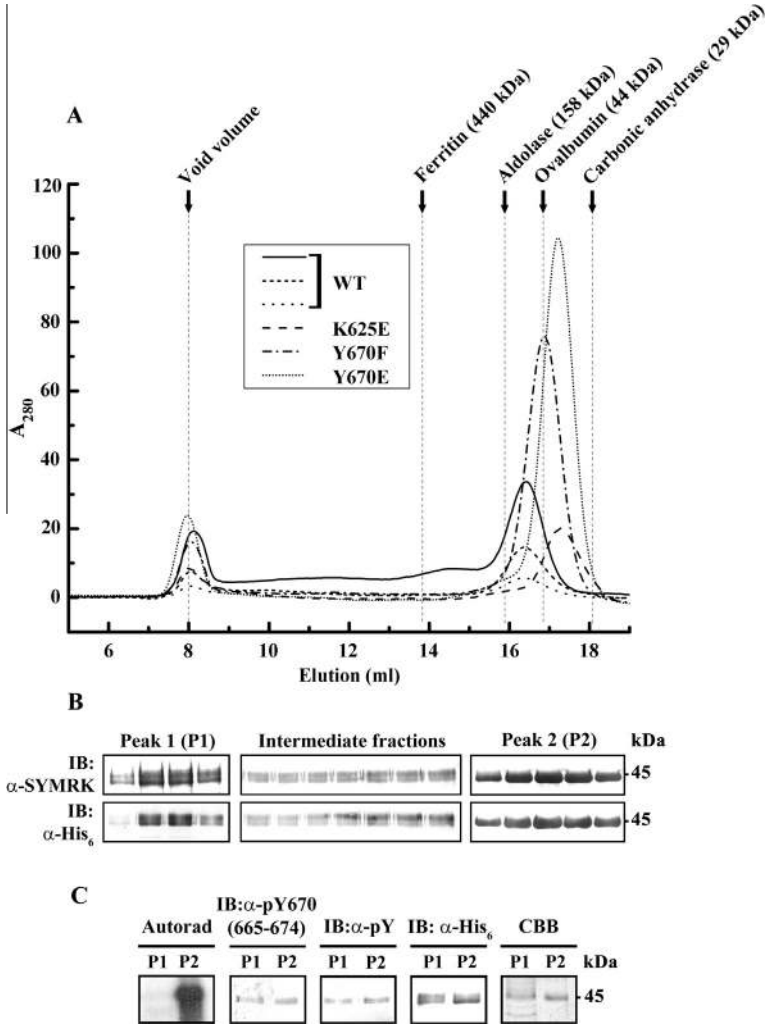

Fig. 3. Size exclusion chromatography of *Ah*SYMRK polypeptides. (A) The Superose-6 FPLC absorbance profile at 280 nm for WT *Ah*SYMRK at increasing concentrations: 8 μM····, 38 μM——— and 75 μM—. The absorbance profiles are also shown for *Ah*SYMRK mutants: K625E– – –, Y670F–·–·– and Y670E·····. The elution behaviour and the apparent molecular mass of marker proteins separated on this column are shown above. Apparent molecular weights of *Ah*SYMRK polypeptides were estimated from the calibration curve (Supplemental Fig. S1). (B) Immunoblot analysis of FPLC purified fractions (P1, intermediate and P2) with α-SYMRK and α-His_6 antibodies. (C) Autophosphorylation of FPLC purified peak 1 (P1) and peak 2 (P2) fractions containing *Ah*SYMRK; from left to right, Autoradiograph of autophosphorylation, immunoblot analysis with α-pY670 (665–674), α-pY, and α-His_6.

Fig. S1). Y670F, which defines a highly active state of the kinase, eluted at 16.86 ml with a slightly higher calculated molecular weight of 44 kDa indicating a change in hydrodynamic properties associated with the active state of this mutant as compared to the inactive Y670E and the K625E mutants. We also noted that the yield of aggregates in the void region was considerably low in Y670E and Y670F as compared to their monomeric form indicating that the tendency to oligomerise was largely decreased in gatekeeper mutated polypeptides.

In this section we demonstrated that native *Ah*SYMRK exists as active homodimers and possesses an intrinsic propensity to form catalytically inactive higher-order oligomers. Unlike BRI1, where deletion of either JM or CT segments abolished dimer formation [12], *Ah*SYMRK kinase domain without its JM and CT segments was sufficient to form stable dimers. However substitution of gatekeeper tyrosine in Y670E and Y670F mutants of *Ah*SYMRK rendered the kinase monomeric with decreased or no propensity to oligomerise. This clearly indicates that presence of tyrosine in the gatekeeper position is important for dimerisation as well as oligomerisation of *Ah*SYMRK. The effect of gatekeeper tyrosine in dimerisation/oligomerisation could be mediated through conformations of the kinase resulting from its hydrogen-bond interactions with the conserved Lys/Glu salt-bridge (K625/E641) which would be destabilised in both the gatekeeper mutants (Y670E and Y670F) as well as the K625E mutant rendering them monomeric. Alternatively, since the catalytically dead K625E mutant failed to dimerise, it is possible that an active kinase autophosphorylated in key positions including the gatekeeper tyrosine is necessary for dimerisation. Intriguingly, BRI1 kinase without its JM domain not only fails to oligomerise but also fails to autophosphorylate on Tyr [12,14], implying the importance of Tyr phosphorylation in determining the oligomeric state of an RLK. The exact structural features contributing to the dimerisation process of *Ah*SYMRK however remain to be ascertained in future experiments.

3.4. *AhSYMRK phosphorylated on gatekeeper tyrosine is inactive*

Our next objective was to directly demonstrate the effect of gatekeeper phosphorylation on the catalytic activity of *Ah*SYMRK in the native polypeptide. For this we enriched the pTyr-containing *Ah*SYMRK by immuno-fractionation using α-pTyr (Fig. 4). The sequentially immunoprecipitated *Ah*SYMRK (Bound1 and Bound2) and the corresponding unbound fractions (Unbound1 and

Unbound2) represented the pTyr-enriched and depleted fractions, respectively. Only a small fraction (<10%) of *Ah*SYMRK could be immuno-precipitated with α-pTyr (Fig. 4A). The poor immuno-precipitation of the gatekeeper-phosphorylated *Ah*SYMRK could be due to the relative inaccessibility of pY670. Immunoblot analysis using α-pY670 (665–674) indicated that there was ~three-fold enrichment of pY670 in 'Bound' fraction (pY670-enriched) whereas only a two-fold reduction in the 'Unbound' fraction (pY670-depleted) when compared to native *Ah*SYMRK (Fig. 4A). The pY670-enriched and pY670-depleted His_6-*Ah*SYMRK fractions were subjected to *in vitro* autophosphorylation in presence of [γ-^{32}P]-ATP as described in experimental procedures. As indicated in Fig. 4B, the pY670-enriched form was barely active compared to the pY670-depleted form, indicating that the pY670-containing *Ah*SYMRK represents an inactive form of the kinase. This inactivation could be due to introduction of charge in the ATP-binding cleft that has a destabilizing effect similar to Y670E mutant. Introducing a positive charge in the same position by substituting the gatekeeper threonine with lysine has been shown to inactivate Src kinase [6] suggesting that charged residues in the hydrophobic pocket deep within the active site destabilize the catalytic groove. In addition, phosphorylation on the gatekeeper residue can affect the hydrophobic connectivity in the catalytic spine of the kinase to inactivate it [4,6]. A charged residue in the gatekeeper position could also interfere with the relative orientations of the two lobes in *Ah*SYMRK by interfering with its hinge-bending motions [30]. Whatever be the underlying mechanism of inactivation, our results clearly indicate that autophosphorylation on the gatekeeper Tyr (Y670) inactivates *Ah*SYMRK and suggests an important role of phosphorylation/dephosphorylation of gatekeeper tyrosine in determining the catalytic output of *Ah*SYMRK.

3.5. Activation of intramolecular autophosphorylation in pY670-depleted AhSYMRK

We next attempted to compare the catalytic activity of native *Ah*SYMRK with its pY670-depleted form (Unbound, Fig. 4A). For this, we monitored the progress of *in vitro* autophosphorylation of

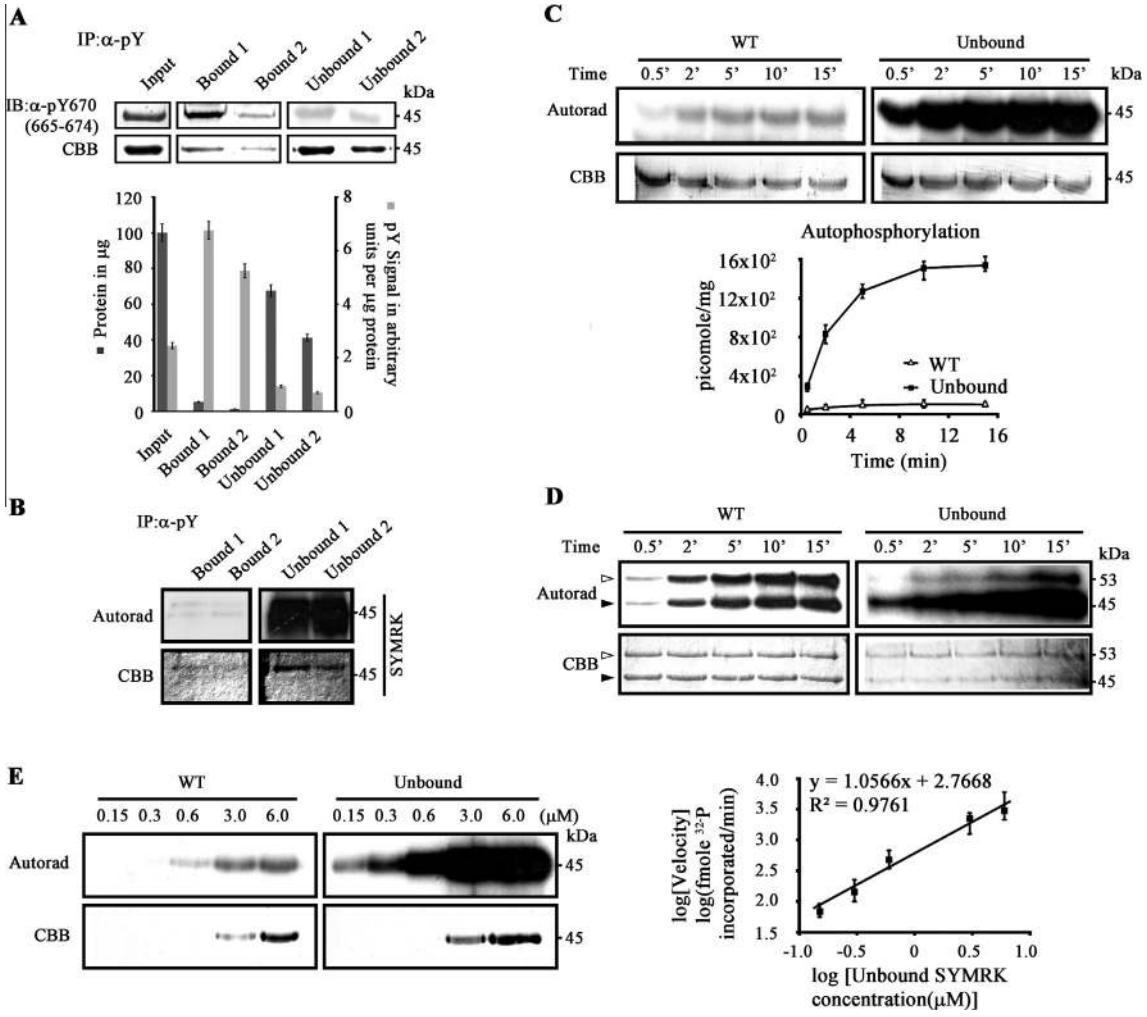

Fig. 4. *Ah*SYMRK phosphorylated on gatekeeper tyrosine is inactive and inhibitory. (A) Enrichment of pTyr-containing *Ah*SYMRK by sequential immunoprecipitation (IP): pY670-enriched (Bound1 and Bound2) and pY670-depleted (Unbound1 and Unbound 2) *Ah*SYMRK were subjected to immunoblot analysis using α-pY670 (665–674) (*upper panel*) and subjected to normalized densitometry (*lower panel*). Data are presented as means ± SEM (n = 3 experiments). (B) Autophosphorylation potential of pY670-enriched *Ah*SYMRK: representative autoradiographs of autophosphorylation by the indicated Bound and Unbound fractions. (C) Comparison of the catalytic potential of native *Ah*SYMRK (WT) and pY670-depleted *Ah*SYMRK (Unbound): (C, *upper panel*) WT *Ah*SYMRK and pY670-depleted *Ah*SYMRK (Unbound) were subjected to autophosphorylation for indicated time points: representative autoradiograph indicating the progress of autophosphorylation. (C, *lower panel*) Densitometric analysis where the data are presented as means ± SEM (n = 3 experiments). (D) Progress of intermolecular autophosphorylation of Trx-K625E (53 kDa) by native WT *Ah*SYMRK (45 kDa) and pY670-depleted *Ah*SYMRK (Unbound, 45 kDa): white and black arrowheads beside the autoradiographs indicate the positions of Trx-K625E and *Ah*SYMRK, respectively. (E) Effect of enzyme concentration on the autophosphorylation potential of native *Ah*SYMRK (WT) and pY670-depleted *Ah*SYMRK (Unbound): autoradiograph (*left panel*) and van't Hoff plot of the log of velocity versus the log of enzyme concentration where the data were produced by scintillation counting and are represented as means ± SEM (n = 3 experiments) (*right panel*).

*Ah*SYMRK and the pY670-depleted fractions where autophosphorylation was noted to be significantly higher in the pY670-depleted *Ah*SYMRK fraction (Fig. 4C). By estimating the radioactivity incorporated in the corresponding bands it was found that there was ~15-fold increase in the autophosphorylation level by the depletion of pY670-*Ah*SYMRK from the native preparation (Fig. 4C). The ~two-fold reduction of the inactive form of the pY670-containing *Ah*SYMRK in the depleted fraction (Fig. 4A) could not account for the ~15-fold increase in autophosphorylation of the pY670-depleted *Ah*SYMRK fraction (Fig. 4C) and suggested that pY670 inhibited autophosphorylation activity of the kinase. Or in other words, phosphorylation on gatekeeper tyrosine appeared to be autoinhibitory.

Like several other RLKs, *Ah*SYMRK autophosphorylated in both an intra and intermolecular manner [43–45]. Our next objective was to understand whether the observed inhibition was targeted to intra or intermolecular autophosphorylation or both. For that similar progress curves of the native and the pY670-depleted *Ah*SYMRK were developed in the presence of the catalytically dead kinase (Trx-K625E-*Ah*SYMRK). As shown in Fig. 4D, the increased autophosphorylation on the pY670-depleted *Ah*SYMRK was intramolecular as phosphorylation on Trx-K625E-*Ah*SYMRK mutant remained relatively unaffected by depletion of pY670-containing *Ah*SYMRK. However, these results did not eliminate the possibility of hierarchical or processive intermolecular autophosphorylation events that could only be undertaken by an active kinase [46]. To clarify this possibility, we analysed autophosphorylation by the pY670-depleted *Ah*SYMRK fraction over a series of dilutions (up to 40-fold) (Fig. 4E). van't Hoff analysis of the data using linear regression produced a slope of 1.05 with a correlation coefficient of 0.97 indicating the mechanism of increased self-phosphorylation of the kinase by pY670 depletion to be intramolecular. Based on these findings, we conclude that autophosphorylation on gatekeeper tyrosine was autoinhibitory towards intramolecular autophosphorylation undertaken by active *Ah*SYMRK. Overall, data in this section show autophosphorylation on gatekeeper tyrosine to impede the activity of *Ah*SYMRK.

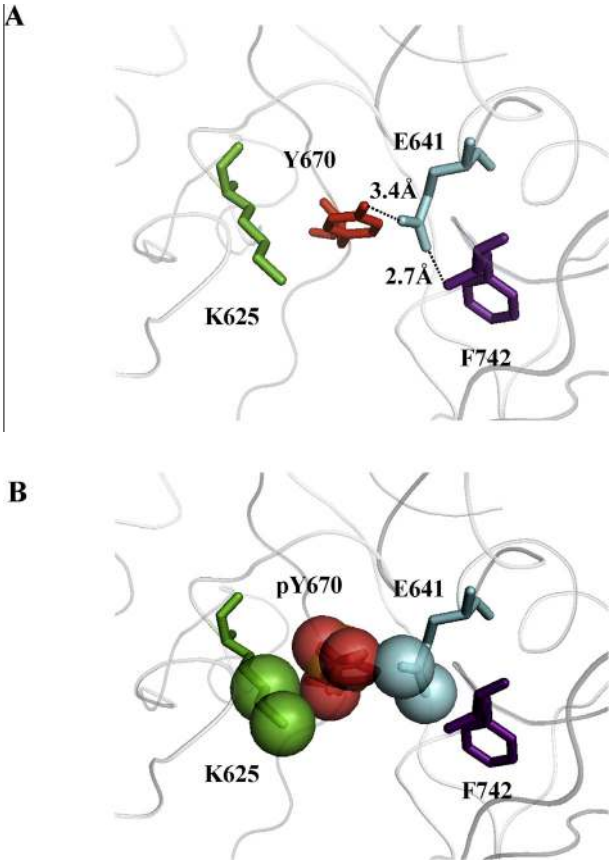

Fig. 5. Proposed model for gatekeeper phosphorylation mediated inactivation of *Ah*SYMRK. (A) In a homology model (generated on 2OID_B, Supplemental Fig. S2), Y670 (red), the invariant glutamate from α-helix C (E641, cyan) and the aspartate from DFG motif (F742, violet) are in H-bonding distance which is a signature of an active conformation for several kinases [9]. The corresponding distances between these residues are also indicated. (B) A simulated phosphate moiety on Y670 appeared to clash with E641 and K625 resulting in probable destabilization of the active site.

4. Summary

*Ah*SYMRK autophosphorylated on gatekeeper tyrosine though phosphorylation on this site was not necessary for the kinase activity [17]. In this report we demonstrate that gatekeeper tyrosine autophosphorylation (pY670) inactivated *Ah*SYMRK. To demonstrate how phosphorylation on the gatekeeper Tyr (pY670) might influence the architecture of the catalytic groove, we developed a homology model of *Ah*SYMRK based on IRAK4 (PDB ID: 2OID_B) (Supplemental Fig. S2). As indicated in Fig. 5A, the conserved Glu (E641) in α-helix C appeared to be within H-bonding distance with Y670 as well as with the backbone of a Phe residue (F742) in the DFG motif of the activation segment. The corresponding residues in IRAK4 (2OID_B) forms a H-bonding network that is considered to be a signature of the activated state of both IRAK4 [10,11] and other RLKs [9]. Insertion of a phosphate group on gatekeeper Tyr (Y670) in *Ah*SYMRK model indicates a probable steric clash and charge repulsion with E641 in α-helix C (Fig. 5B) which could disorganise the H-bond network and uncouple the salt-bridge interaction between E641 with K625. This destabilisation of the catalytic groove is a plausible explanation for the strong reduction of catalytic activity in *Ah*SYMRK phosphorylated in gatekeeper tyrosine.

In addition, depletion of the gatekeeper phosphorylated inactive form of *Ah*SYMRK activated intramolecular autophosphorylation of the kinase suggesting gatekeeper tyrosine phosphorylation to have an autoinhibitory effect on this RLK. This is the first report of gatekeeper phosphorylation mediated inhibition of protein kinases that adds another evidence in favour of hinge region having an important role in autoinhibition of protein kinases. Usually, autoinhibitory domains are localized outside the kinase domain [47,48] but several evidences indicate the role of hinge region within the kinase domain to have an autoinhibitory effect on protein kinases. These evidences include (i) autoinhibitory network of H-bonds at the hinge region known as a 'molecular brake' in RTKs [49], (ii) intramolecular autoinhibitory interaction of αC-β4 loop with activation loop of ErbB2 receptor kinase [50], (iii) autoinhibited conformation of the GCN2 by an arginine residue mediated rigidification of hinge region [51], (iv) autoinhibition of NEK7 kinase by preventing the interaction of its gatekeeper leucine with another leucine in the αC loop [52], (v) a cluster of hydrophobic residues that interact with the gatekeeper form a novel structural unit that restrain backbone flexibility at the activation loop through an intramolecular pathway of connectivity in ERK2 [7]. Therefore it appears that the hinge region alongwith the gatekeeper serves as a potential mediator of autoinhibition in protein kinases. Since presence of a gatekeeper tyrosine residue is a conserved feature in RLKs, it remains to be seen whether phosphorylation on gatekeeper tyrosine and its autoinhibitory effects are of widespread occurrence in RLKs.

Conflict of interest

The authors declare that they have no conflict of interest.

Acknowledgements

This work was supported by Grants from Govt. of India (i) DBT CEIB (BT/01/CEIB/09/VI/10) (ii) DBT-IPLS (BT/PR14552/INF/22/123/2010). We thank UGC for providing fellowships to A.P., S.S., A.B., CSIR for A.B. and ICMR for A.D. We also thank CSIR-IICB and DBT, India for infrastructural support and the Ramalingaswami fellowship, respectively to S.C.

Appendix A. Supplementary data

Supplementary data associated with this article can be found, in the online version, at http://dx.doi.org/10.1016/j.febslet.2014.06.056.

References

[1] Kornev, A.P. and Taylor, S.S. (2010) Defining the conserved internal architecture of a protein kinase. Biochim. Biophys. Acta 1804, 440–444.
[2] Lindin, I., Wuxiuer, Y., Ravna, A.W., Moens, U. and Sylte, I. (2014) Comparative molecular dynamics simulations of mitogen-activated protein kinase-activated protein kinase 5. Int. J. Mol. Sci. 15, 4878–4902.
[3] Zuccotto, F., Ardini, E., Casale, E. and Angiolini, M. (2010) Through the "gatekeeper door": exploiting the active kinase conformation. J. Med. Chem. 53, 2681–2694.
[4] Taylor, S.S. and Kornev, A.P. (2011) Protein kinases: evolution of dynamic regulatory proteins. Trends Biochem. Sci. 36, 65–77.
[5] Liu, Y., Shah, K., Yang, F., Witucki, L. and Shokat, K.M. (1998) A molecular gate which controls unnatural ATP analogue recognition by the tyrosine kinase v-Src. Bioorg. Med. Chem. 6, 1219–1226.
[6] Azam, M., Seeliger, M.A., Gray, N.S., Kuriyan, J. and Daley, G.Q. (2008) Activation of tyrosine kinases by mutation of the gatekeeper threonine. Nat. Struct. Mol. Biol. 15, 1109–1118.
[7] Emrick, M.A., Lee, T., Starkey, P.J., Mumby, M.C., Resing, K.A. and Ahn, N.G. (2006) The gatekeeper residue controls autoactivation of ERK2 via a pathway of intramolecular connectivity. Proc. Natl. Acad. Sci. USA 103, 18101–18106.
[8] Sours, K.M., Xiao, Y. and Ahn, N.G. (2014) Extracellular-regulated kinase 2 is activated by the enhancement of hinge flexibility. J. Mol. Biol..
[9] Klaus-Heisen, D. et al. (2011) Structure–function similarities between a plant receptor-like kinase and the human interleukin-1 receptor-associated kinase-4. J. Biol. Chem. 286, 11202–11210.
[10] Wang, Z., Liu, J., Sudom, A., Ayres, M., Li, S., Wesche, H., Powers, J.P. and Walker, N.P. (2006) Crystal structures of IRAK-4 kinase in complex with inhibitors: a serine/threonine kinase with tyrosine as a gatekeeper. Structure 14, 1835–1844.
[11] Kuglstatter, A. et al. (2007) Cutting Edge: IL-1 receptor-associated kinase 4 structures reveal novel features and multiple conformations. J. Immunol. 178, 2641–2645.
[12] Bojar, D., Martinez, J., Santiago, J., Rybin, V., Bayliss, R. and Hothorn, M. (2014) Crystal structures of the phosphorylated BRI1 kinase domain and implications for brassinosteroid signal initiation. Plant J. 78, 31–43.
[13] Yan, L. et al. (2012) Structural basis for the impact of phosphorylation on the activation of plant receptor-like kinase BAK1. Cell Res. 22, 1304–1308.
[14] Oh, M.H., Wang, X., Kota, U., Goshe, M.B., Clouse, S.D. and Huber, S.C. (2009) Tyrosine phosphorylation of the BRI1 receptor kinase emerges as a component of brassinosteroid signaling in Arabidopsis. Proc. Natl. Acad. Sci. USA 106, 658–663.
[15] Lin, W., Li, B., Lu, D., Chen, S., Zhu, N., He, P. and Shan, L. (2014) Tyrosine phosphorylation of protein kinase complex BAK1/BIK1 mediates Arabidopsis innate immunity. Proc. Natl. Acad. Sci. USA 111, 3632–3637.
[16] Oh, M.H., Wang, X., Wu, X., Zhao, Y., Clouse, S.D. and Huber, S.C. (2010) Autophosphorylation of Tyr-610 in the receptor kinase BAK1 plays a role in brassinosteroid signaling and basal defense gene expression. Proc. Natl. Acad. Sci. USA 107, 17827–17832.
[17] Samaddar, S. et al. (2013) Autophosphorylation of gatekeeper tyrosine by symbiosis receptor kinase. FEBS Lett. 587, 2972–2979.
[18] Stracke, S. et al. (2002) A plant receptor-like kinase required for both bacterial and fungal symbiosis. Nature 417, 959–962.
[19] Endre, G., Kereszt, A., Kevei, Z., Mihacea, S., Kalo, P. and Kiss, G.B. (2002) A receptor kinase gene regulating symbiotic nodule development. Nature 417, 962–966.
[20] Dasgupta, M., Honeycutt, T. and Blumenthal, D.K. (1989) The gamma-subunit of skeletal muscle phosphorylase kinase contains two noncontiguous domains that act in concert to bind calmodulin. J. Biol. Chem. 264, 17156–17163.
[21] DasGupta, M. (1994) Characterization of a calcium-dependent protein kinase from *Arachis hypogea* (groundnut) seeds. Plant Physiol. 104, 961–969.
[22] Raichaudhuri, A., Bhattacharyya, R., Chaudhuri, S., Chakrabarti, P. and Dasgupta, M. (2006) Domain analysis of a groundnut calcium-dependent protein kinase: nuclear localization sequence in the junction domain is coupled with nonconsensus calcium binding domains. J. Biol. Chem. 281, 10399–10409.
[23] Kelly, S.M., Jess, T.J. and Price, N.C. (2005) How to study proteins by circular dichroism. Biochim. Biophys. Acta 1751, 119–139.
[24] Meyer, M.R., Lichti, C.F., Townsend, R.R. and Rao, A.G. (2011) Identification of in vitro autophosphorylation sites and effects of phosphorylation on the Arabidopsis CRINKLY4 (ACR4) receptor-like kinase intracellular domain: insights into conformation, oligomerization, and activity. Biochemistry 50, 2170–2186.
[25] Hildebrand, A., Remmert, M., Biegert, A. and Soding, J. (2009) Fast and accurate automatic structure prediction with HHpred. Proteins 77 (Suppl. 9), 128–132.
[26] Eswar, N., Eramian, D., Webb, B., Shen, M.Y. and Sali, A. (2008) Protein structure modeling with MODELLER. Methods Mol. Biol. 426, 145–159.
[27] Laskowski, R.A., MacArthur, M.W., Moss, D.S. and Thornton, J.M. (1993) PROCHECK: a program to check the stereochemical quality of protein structures. J. Appl. Crystallogr. 26, 283–291.
[28] Eisenberg, D., Luthy, R. and Bowie, J.U. (1997) VERIFY3D: assessment of protein models with three-dimensional profiles. Methods Enzymol. 277, 396–404.
[29] Pettersen, E.F., Goddard, T.D., Huang, C.C., Couch, G.S., Greenblatt, D.M., Meng, E.C. and Ferrin, T.E. (2004) UCSF Chimera – a visualization system for exploratory research and analysis. J. Comput. Chem. 25, 1605–1612.
[30] Jura, N., Zhang, X., Endres, N.F., Seeliger, M.A., Schindler, T. and Kuriyan, J. (2011) Catalytic control in the EGF receptor and its connection to general kinase regulatory mechanisms. Mol. Cell 42, 9–22.
[31] Wente, S.R., Villalba, M., Schramm, V.L. and Rosen, O.M. (1990) Mn2(+)-binding properties of a recombinant protein-tyrosine kinase derived from the human insulin receptor. Proc. Natl. Acad. Sci. USA 87, 2805–2809.
[32] Sierke, S.L., Cheng, K., Kim, H.H. and Koland, J.G. (1997) Biochemical characterization of the protein tyrosine kinase homology domain of the ErbB3 (HER3) receptor protein. Biochem. J. 322 (Pt 3), 757–763.
[33] Fontana, A., de Laureto, P.P., Spolaore, B., Frare, E., Picotti, P. and Zambonin, M. (2004) Probing protein structure by limited proteolysis. Acta Biochim. Pol. 51, 299–321.
[34] Gadella Jr., T.W. and Jovin, T.M. (1995) Oligomerization of epidermal growth factor receptors on A431 cells studied by time-resolved fluorescence imaging microscopy. A stereochemical model for tyrosine kinase receptor activation. J. Cell Biol. 129, 1543–1558.
[35] Livnah, O., Stura, E.A., Middleton, S.A., Johnson, D.L., Jolliffe, L.K. and Wilson, I.A. (1999) Crystallographic evidence for preformed dimers of erythropoietin receptor before ligand activation. Science 283, 987–990.
[36] Moriki, T., Maruyama, H. and Maruyama, I.N. (2001) Activation of preformed EGF receptor dimers by ligand-induced rotation of the transmembrane domain. J. Mol. Biol. 311, 1011–1026.
[37] Mischel, P.S., Umbach, J.A., Eskandari, S., Smith, S.G., Gundersen, C.B. and Zampighi, G.A. (2002) Nerve growth factor signals via preexisting TrkA receptor oligomers. Biophys. J. 83, 968–976.
[38] Ferguson, K.M., Berger, M.B., Mendrola, J.M., Cho, H.S., Leahy, D.J. and Lemmon, M.A. (2003) EGF activates its receptor by removing interactions that autoinhibit ectodomain dimerization. Mol. Cell 11, 507–517.
[39] Russinova, E., Borst, J.W., Kwaaitaal, M., Cano-Delgado, A., Yin, Y., Chory, J. and de Vries, S.C. (2004) Heterodimerization and endocytosis of Arabidopsis brassinosteroid receptors BRI1 and AtSERK3 (BAK1). Plant Cell 16, 3216–3229.
[40] Wang, X. et al. (2005) Identification and functional analysis of in vivo phosphorylation sites of the Arabidopsis BRASSINOSTEROID-INSENSITIVE1 receptor kinase. Plant Cell 17, 1685–1703.
[41] Hink, M.A., Shah, K., Russinova, E., de Vries, S.C. and Visser, A.J. (2008) Fluorescence fluctuation analysis of *Arabidopsis thaliana* somatic embryogenesis receptor-like kinase and brassinosteroid insensitive 1 receptor oligomerization. Biophys. J. 94, 1052–1062.
[42] Giranton, J.L., Dumas, C., Cock, J.M. and Gaude, T. (2000) The integral membrane S-locus receptor kinase of Brassica has serine/threonine kinase activity in a membranous environment and spontaneously forms oligomers in planta. Proc. Natl. Acad. Sci. USA 97, 3759–3764.
[43] Oh, M.H., Ray, W.K., Huber, S.C., Asara, J.M., Gage, D.A. and Clouse, S.D. (2000) Recombinant brassinosteroid insensitive 1 receptor-like kinase autophosphorylates on serine and threonine residues and phosphorylates a conserved peptide motif in vitro. Plant Physiol. 124, 751–766.
[44] Liu, G.Z., Pi, L.Y., Walker, J.C., Ronald, P.C. and Song, W.Y. (2002) Biochemical characterization of the kinase domain of the rice disease resistance receptor-like kinase XA21. J. Biol. Chem. 277, 20264–20269.
[45] Schulze-Muth, P., Irmler, S., Schroder, G. and Schroder, J. (1996) Novel type of receptor-like protein kinase from a higher plant (*Catharanthus roseus*). cDNA, gene, intramolecular autophosphorylation, and identification of a threonine important for auto- and substrate phosphorylation. J. Biol. Chem. 271, 26684–26689.
[46] Lew, E.D., Furdui, C.M., Anderson, K.S. and Schlessinger, J. (2009) The precise sequence of FGF receptor autophosphorylation is kinetically driven and is disrupted by oncogenic mutations. Sci. Signal. 2, ra6.
[47] Smock, R.G. and Gierasch, L.M. (2009) Sending signals dynamically. Science 324, 198–203.
[48] Nagar, B. et al. (2003) Structural basis for the autoinhibition of c-Abl tyrosine kinase. Cell 112, 859–871.
[49] Chen, H., Ma, J., Li, W., Eliseenkova, A.V., Xu, C., Neubert, T.A., Miller, W.T. and Mohammadi, M. (2007) A molecular brake in the kinase hinge region regulates the activity of receptor tyrosine kinases. Mol. Cell 27, 717–730.

[50] Fan, Y.X., Wong, L., Ding, J., Spiridonov, N.A., Johnson, R.C. and Johnson, G.R. (2008) Mutational activation of ErbB2 reveals a new protein kinase autoinhibition mechanism. J. Biol. Chem. 283, 1588–1596.
[51] Padyana, A.K., Qiu, H., Roll-Mecak, A., Hinnebusch, A.G. and Burley, S.K. (2005) Structural basis for autoinhibition and mutational activation of eukaryotic initiation factor 2alpha protein kinase GCN2. J. Biol. Chem. 280, 29289–29299.
[52] Richards, M.W., O'Regan, L., Mas-Droux, C., Blot, J.M., Cheung, J., Hoelder, S., Fry, A.M. and Bayliss, R. (2009) An autoinhibitory tyrosine motif in the cell-cycle-regulated Nek7 kinase is released through binding of Nek9. Mol. Cell 36, 560–570.